

Learning Latent Graph Dynamics for Visual Manipulation of Deformable Objects

Xiao Ma, David Hsu, *Fellow, IEEE*, and Wee Sun Lee

Abstract—Manipulating deformable objects, such as ropes and clothing, is a long-standing challenge in robotics, because of their large degrees of freedom, complex non-linear dynamics, and self-occlusion in visual perception. The key difficulty is a suitable representation, rich enough to capture the object shape, dynamics for manipulation and yet simple enough to be estimated reliably from visual observations. This work aims to learn latent *Graph dynamics for DefOrmable Object Manipulation* (G-DOOM). G-DOOM approximates a deformable object as a sparse set of interacting *keypoints*, which are extracted automatically from images via unsupervised learning. It learns a *graph neural network* that captures abstractly the geometry and the interaction dynamics of the keypoints. To handle object self-occlusion, G-DOOM uses a recurrent neural network to track the keypoints over time and condition their interactions on the history. We then train the resulting recurrent graph dynamics model through contrastive learning in a high-fidelity simulator. For manipulation planning, G-DOOM reasons explicitly about the learned dynamics model through model-predictive control applied at each keypoint. Preliminary experiments of G-DOOM on a set of challenging rope and cloth manipulation tasks indicate strong performance, compared with state-of-the-art methods. Although trained in a simulator, G-DOOM transfers directly to a real robot for both rope and cloth manipulation¹.

Index Terms—Deformable object manipulation, graph neural networks

I. INTRODUCTION

Robot manipulation of rigid-body objects has made significant progress in recent years, but many manipulation tasks in daily life involve deformable objects, *e.g.*, pulling cables, folding clothes, or bagging groceries. Manipulating deformable objects remains an open challenge because of their large degrees of freedom, complex non-linear dynamics, and self-occlusion in visual perception.

Early work on deformable object manipulation uses predefined visual features to capture the object shape and plans robot actions with handcrafted approximate dynamics models [17, 23, 28]. Predefined geometric features are often not robust and introduce errors in state estimation. The approximate dynamics model then compounds the error during long-horizon planning [6, 15]. Recent data-driven methods shun explicit modeling and learn policies that directly map raw visual observations to robot actions [16, 25, 32]. Models, however,

The authors are with the School of Computing, National University of Singapore. Email: {xiao-ma, dyhsu, leews}@comp.nus.edu.sg

This research is supported in part by the National Research Foundation (NRF), Singapore under its AI Singapore Program (AISG Award No: AISG2-RP-2020-016) and by the Agency of Science, Technology & Research, Singapore, through the National Robotics Program (Grant No. 192 25 00054).

¹Demo video available online at <https://youtu.be/oCfbNMx2sQI>

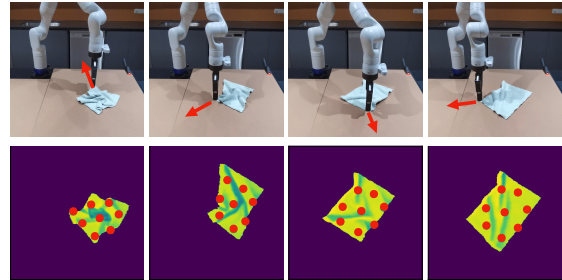


Fig. 1. G-DOOM flattens a piece of crumpled cloth in 4 steps, using a Kinova Gen3 robot. It reasons about a learned graph dynamics model over keypoints (bottom row), which are extracted from depth images. The red arrows (top row) indicate robot actions.

provide strong inductive bias for learning and improve generalization. Some recent methods use the particle representation and successfully learn dynamics models for complex non-rigid objects, *e.g.*, fluids [11, 24, 1], but they require a large number of particles for accurate dynamics prediction. The resulting high computational cost makes them unsuitable for real-time manipulation planning.

We hypothesize that while models of object shapes and dynamics are crucial for manipulation planning, high model accuracy may be unnecessary for many manipulation tasks in daily life. Consider how humans fold a piece of clothing. Instead of accurately reasoning the dynamics of every point on the clothing, we focus only on a few *keypoints*, the collar, shoulders, *etc.*, which are easy to observe visually and sufficient to capture the key underlying dynamics information abstractly.

To this end, we present *latent Graph dynamics for DefOrmable Object Manipulation* (G-DOOM), a new method for visual manipulation of deformable objects. G-DOOM approximates a deformable object as a *sparse* set of interacting keypoints (Fig. 1). It consists of three components. First, G-DOOM extracts from depth images a set of visually-salient keypoint features, via unsupervised learning [8]. Second, G-DOOM learns a *recurrent graph neural network* model to capture the complex non-linear dynamics of keypoints. It represents each keypoint as a node in a graph neural network (GNN) [33] and applies graph convolution on the keypoint features to learn “summaries” of the keypoint interactions abstractly. To handle object self-occlusion, it further makes the GNN recurrent and conditions the keypoint interaction model on the history. Unlike the humans who track a set of fixed keypoints, G-DOOM does not track the keypoints individually at each time step. Instead, it tracks the global statistics of the *keypoint set* and uses them to reason about the dynamics of

the deformable object at an abstract level. Finally, G-DOOM exploits the learned graph dynamics model and applies model-predictive control (MPC) at each keypoint to choose the best action for manipulation.

We evaluated G-DOOM on three deformable manipulation tasks: rope straightening, cloth flattening, and cloth folding. Experiments show that in a high-fidelity simulator, Nvidia Flex [2], G-DOOM outperforms PlaNet [4] and CFM [35], the state-of-the-art method for visual manipulation of deformable objects. While G-DOOM is trained entirely in simulation, it transfers directly to a Kinova Gen3 robot for both rope and cloth manipulation. The experimental results provide the initial evidence to support our hypothesis: a sparse set of keypoints can capture the dynamics of a complex deformable object.

II. RELATED WORKS

Early work on deformable object manipulation uses predefined visual features for object state estimation [10, 34] and plans with handcrafted approximate dynamics models, *e.g.*, linear models [19, 23, 27, 31]. One major difficulty is a powerful representation that connects rich visual perception and complex object dynamics for long-horizon robot manipulation planning. The recent advances in data-driven methods, especially, deep learning, have brought up significant interests in learning model-free policies [16, 18, 32, 9, 3] or dynamics models [4, 14, 35] from raw visual images. However, a lot of prior works on model learning use the unstructured state representation as a single vector (see, *e.g.*, [6, 15]). Structured representations, such as particles [11, 24] or graphs [7, 11, 26, 36, 37], generally improve the predictive power and generalization capability of the learned models. Hence, G-DOOM uses a learned graph by GNNs to represent the object’s dynamic state.

Our work follows the general idea of learning latent dynamics models for planning, but focuses on the structured, learnable dynamics representation over a sparse set of visual keypoints. Compared with model-free methods, G-DOOM benefits from the structural inductive bias of the graph dynamics model for generalization. At the same time, it is comparable in computational efficiency with methods using the simpler vector-based state representation for learning. Concurrent to this work, Lin *et al.* [13] propose to learn a visual connectivity graph for cloth smoothing. It represents the cloth as a dense point cloud and tries to reconstruct its 3-D geometry partially. In contrast, G-DOOM demonstrates a learned latent representation over sparse visual keypoints in the image space. The implication is that the overall object shape rather than accurate 3-D shape reconstruction is important for manipulation, at least, in some common daily tasks.

III. G-DOOM

G-DOOM performs visual manipulation of deformable objects, using a learned graph dynamics model over a set of keypoints. Given a top-down image, G-DOOM extracts visually-salient keypoint features, through unsupervised learning. These keypoints represent partial observations of the underlying object state. Specifically, we use depth images

as the input to minimize the sim-to-real gap. Next, to estimate the object state, G-DOOM uses a learned graph dynamics model (Fig. 2) to track a *belief*, *i.e.*, the sufficient statistics of the keypoints. Using the same dynamics model, G-DOOM performs MPC conditioned on the detected keypoints to choose the best action. The main components of G-DOOM—learning keypoint extraction, learning the graph dynamics model, and model predictive control with the learned dynamics model—are described respectively in the three subsections below.

A. Visual Keypoint Extraction

Since manually defining keypoints generalizes poorly to unseen configurations and objects, we leverage the Transporter Networks [8] for unsupervised keypoint detection and feature extraction. The core idea of Transporter Networks is that the salient keypoints should contain sufficient information for pixel-level image reconstruction. During training, we take a pair of images sampled from the a collected dataset, (I_{src}, I_{tgt}) , pass them through a feature extractor f_{enc} and keypoint detector f_{kp} , which gives image features (ϕ_{src}, ϕ_{tgt}) and keypoint heatmaps $(\mathcal{H}_{src}, \mathcal{H}_{tgt})$. The method applies a *transport* operation that composes the local target features ϕ_{tgt} around target keypoints \mathcal{H}_{tgt} into the source feature map ϕ_{src} as $\Psi(\phi_{src}, \phi_{tgt}; \mathcal{H}_{src}, \mathcal{H}_{tgt})$. Given the reconstructed target $\hat{I}_{tgt} = f_{dec}(\Psi(\phi_{src}, \phi_{tgt}; \mathcal{H}_{src}, \mathcal{H}_{tgt}))$, we optimize the keypoint detection module by minimizing the reconstruction loss, $L_{rec} = \| I_{tgt} - \hat{I}_{tgt} \|$.

For an image I_t at time t , we treat the keypoint heatmap \mathcal{H}_t as an attention mask over the feature map ϕ_t and apply mean-pooling over the channel-dimension of ϕ_t . Mathematically, the i -th keypoint feature is computed by $v_t^i = \text{MeanPool}(\mathcal{H}_t^i \phi_t)$, where \mathcal{H}_t^i denotes the i -th channel of the keypoint heatmap. The keypoint location p_t^i can be acquired by $p_t^i = \arg \max \mathcal{H}_t^i$. With depth images as the input, the node feature v_t^i learns to extract the depth and geometric information around position p_t^i , which provides rich information for keypoint interaction modeling. For each image I_t , we construct a graph observation $G_t = (V_t, E_t)$, where $V_t = \{v_t^i\}_{i=1}^K$ and E_t is the set of edges that reflect the *ground-truth* connectivity of the object. In our experiments, we show that the keypoint detector is robust and can be transferred from simulation to real-world images.

B. Recurrent Graph Dynamics

1) *Model Structure*: Given a sequence of top-down images, I_1, I_2, \dots, I_t , the keypoint graph prediction module outputs a sequence of graphs, G_1, G_2, \dots, G_t . Due to the sparsity of keypoints, it remains non-trivial to explicitly model the spatial keypoint interactions with a mathematical model. In addition, the self-occlusion during the deformation of the object introduces partial observability to the task, and eventually makes the exact graph matching between keypoints infeasible.

We present *Recurrent Graph Dynamics* (Fig. 2) to tackle these issues. We parameterize the high-level keypoint interactions among graph G_t using *Graph Neural Networks* and learn the parameters directly from data, which improves the spatial modeling performance over handcrafted models. In addition,

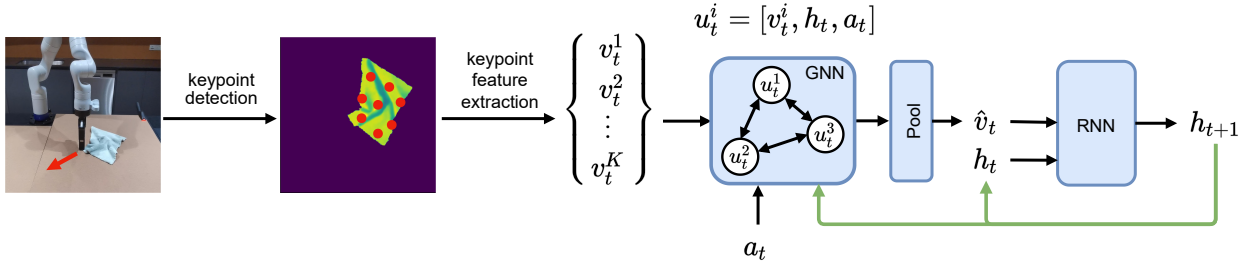


Fig. 2. G-DOOM performs unsupervised keypoint detection on depth images, extracts the corresponding keypoint features $\{v_t^i\}_{i=1}^K$, and compose them into a graph through learned spatial relationships. It learns recurrent graph dynamics to predict the future states with features $\{u_t^i\}_{i=1}^K = \{[v_t^i, h_t, a_t]\}_{i=1}^K$, which account for the spatio-temporal interactions among the local graph features $\{v_t^i\}_{i=1}^K$, an action a_t , and global statistics h_t that captures the history.

instead of performing exact graph matching over the potentially partial keypoint graphs, we propose to extract global features from the graphs, represented by a single vector, and track the *belief* h_t , *i.e.*, the sufficient statistics of the global state (or we can call it the history) of the deformable object, using a recurrent neural network. Such a structure allows us to capture the informative spatial keypoint interactions and effectively estimate the global state of the object over a sequence of partial observations. At each time step t , we update the belief h_t :

$$v_t^i = \text{GNN}([v_t^i, h_t, a_t], \text{Nb}(v_t^i)) \quad (1)$$

$$h_{t+1} = \text{RNN}(h_t, \text{Pool}(\{v_t^i\}_{i=1}^K)) \quad (2)$$

where $\text{Nb}(v_t^i)$ defines the neighbor nodes of v_t^i in graph G_t , Pool is the global pooling operation, and a_t is the action taken. Specifically, in Eqn. 1, by conditioning the spatial feature learning of G_t on the belief h_t , we are able to learn temporally meaningful spatial interactions among keypoints.

However, the visually salient keypoints reveal no underlying connectivity of the object and explicitly defining E_t remains difficult. We propose to learn *soft edges* that indicates the connectivity by a probability w_{ij} through end-to-end learning to maximize the predictive accuracy. We construct a fully connected graph, and rewrite Eqn. 1 as

$$v_t^i = \text{GNN}([v_t^i, h_t, a_t], \{(v_t^j, w_{ij})\}_{j=1}^K) \quad (3)$$

In our implementation, we borrow the idea from Yu *et al.* [36] and use TGConv, a powerful attention-based graph convolution with the powerful Transformer attention mechanisms [29]. In addition, since the keypoints are sparse, standard global mean-pooling or max-pooling might not sufficiently approximate the features of the keypoint set. We augment the pooling operation by *Moment-Generating Function* features [14]. MGF is an alternative specification of a probabilistic distribution. Mathematically, the MGF of a variable \mathbf{X} is defined as $\mathbb{E}[e^{\theta^T \mathbf{X}}]$, $\theta \in \mathbb{R}^n$. MGF features consider θ as a learnable vector and we compute the MGF-pooled feature \hat{v}_t as

$$\hat{v}_t = \text{MGF}(\{v_t^i\}_{i=1}^K) = \left[\frac{1}{K} \sum_{i=1}^K v_t^i, \sum_{i=1}^K e^{\theta^T v_t^i} \right] \quad (4)$$

where $[\cdot, \cdot]$ denotes the concatenation of vectors. Using MGF features, additional higher-order moment features is learned to compensate for the inaccurate Monte-Carlo approximation.

2) *Reward Function*: To allow planning with the learned dynamics, we predict a state-dependent reward by $\hat{r}_t = f_r(\hat{v}_t)$ using a single fully-connected layer f_r with the MGF feature \hat{v}_t , which encodes an ad-hoc and expressive reward signal trained by regressing manually defined rewards.

Alternatively, G-DOOM is capable of goal-oriented manipulation. Given a goal image I_g , G-DOOM extracts the keypoint features $\{v_g^i\}_{i=1}^K$ and construct the MGF feature $\hat{v}_g = \text{MGF}(\{v_g^i\}_{i=1}^K)$. We can define the reward as $r_g = -\|\hat{v} - \hat{v}_g\|_2$, where \hat{v} is the MGF feature of the current state. The goal-oriented reward r_g is more flexible, but less expressive given complex goals, *e.g.*, a rope with a knot. In our experiments, we mainly focus on \hat{r}_t .

3) *Model Learning*: G-DOOM is learned by optimizing a loss function, $L = L_D + \alpha L_R$, where L_D is the dynamics loss, L_R is the reward loss for \hat{r}_t , and α is a hyper-parameter balancing the two objectives.

Given the observation sequence $I_{1:t}$, we unroll the model for $T - t$ steps and predict the graph sequence $\{\hat{v}_{t+1:T}^i\}_{i=1}^K$ using Eqn. 2. For the reward part, we simply train the reward predictor by minimizing the prediction error along the trajectory with $L_R = \sum_{t'=t+1}^T (\hat{r}_{t'} - r_{t'})^2$. For dynamics part, given the observation sequence $I_{1:t}$, we minimize the distance between the predicted graphs and the encoded graphs $\{v_{t+1:T}^i\}_{i=1}^K$ from the future observations $I_{t+1:T}$. To avoid exact graph matching, we instead minimize the distance between the single vector representations, *i.e.*, the MGF-pooled encoded state \hat{v}_t and MGF-pooled encoded state v_t . Similar to *Contrastive Forward Model* (CFM) [35], we adopt a contrastive learning objective to improve the robustness against noisy and complex observations. Different from the standard InfoNCE loss [20], we use an energy-based hinge-loss L_D to improve the robustness of the learned representation against sparse and potentially noisy keypoint detections

$$L_D = \sum_{t'=t+1}^T \left\{ \|\hat{v}_{t'} - v_{t'}\|_2 + \sum_{n=1}^N \max(0, \gamma - \|\hat{v}_{t'} - v_n\|_2) \right\} \quad (5)$$

where $\{v_n\}_{n=1}^N$ are negative states encoded from a set of observations $\{I_n\}_{n=1}^N$ sampled randomly from the datasets.



Fig. 3. Deformable object simulation in NVidia-Flex [2], a high-fidelity particle-based simulator. For each object, both the 3-D visualization and the corresponding depth image are shown.

C. Model-Predictive Control with Learned Graph Dynamics

Throughout our tasks, we use a pick-and-place action, $a = (x_s, y_s, x_g, y_g)$, where (x_s, y_s) is the pick position and (x_g, y_g) is the place position. Inspired by the human cloth folding, we observe that an effective action normally takes effect around the keypoints. We introduce a simple yet effective strategy, graph-based Model-Predictive Control (MPC), where we combine the standard MPC with the hind-sight optimization [5]. The intuition behind is that we initialize K action sequences $\{\mathbf{a}^i\}_{i=1}^K$, centered at the keypoint $p_t^i = (x_t^i, y_t^i)$. In implementation, we initialize the search with K hidden states $\{h_t^i\}_{i=1}^K$, unroll the trajectory with actions $\{\mathbf{a}^i\}_{i=1}^K$ and the learned dynamics (Eqn. 2 and Eqn. 3), and maximize the predicted reward $\{\hat{R}^i = \sum_{t'=t}^{t+T} \hat{r}_{t'}\}_{i=1}^K$. The final action is acquired by $\mathbf{a}^* = \arg \max_{\mathbf{a}^i} \hat{R}^i$. This focuses the search space around the important space and empirically, we can observe a significant performance gain in our experiments.

IV. EXPERIMENTS

We first evaluate the proposed G-DOOM on a set of rope straightening and cloth manipulation tasks in a high-fidelity simulator, NVidia-Flex [2]. To minimize the sim-to-real gap, we use masked depth images as the input, and we show that our learned dynamics model transfers directly to a real robot.

We compare G-DOOM with the state-of-the-art (SOTA) model-based deformable object manipulation method, *Contrastive Forward Model* (CFM) [35], and a SOTA general-purpose model-based RL method, PlaNet [4]. For all baselines, we use publicly available implementations. For a fair comparison, we adapt the original goal-oriented CFM to reward-driven by adding an additional reward predictor.

A. Experiment Setup

1) *Simulation Environment*: We build our simulator upon SoftGym [12], a soft-body simulator based on NVidia-Flex [2], the state-of-the-art (SOTA) particle-based simulator. Example images are shown in Fig. 3. We make certain modifications on SoftGym to better match the real-robot scenarios, where:

- *Observation space*. The observation is a depth image of size 96×96 with depth values, indicating the distance to a top-down simulated camera. Specifically, we perform object segmentation and set the background values to 0.
- *Action space*. As mentioned in Sect. III-C, we use a pick-and-place action, $a_t = [x_s, y_s, x_g, y_g]$, where (x_s, y_s) is the pick position and (x_g, y_g) is the place position.

2) *Tasks*: We evaluate the proposed G-DOOM on 2 cloth manipulation and 4 rope straightening tasks.

- *Rope Straightening*. The task is to straighten a rope and position it at the center of the image with different orientations ($0^\circ, 45^\circ, 90^\circ, 135^\circ$). The challenge is to understand the complex non-linear dynamics of a deformable object.
- *Cloth Manipulation*. The cloth manipulation tasks are more challenging than the rope straightening because of the partial observability caused by self-occlusions. It consists of two sub-tasks: (1) cloth flattening, where the task is to flatten a piece of randomly crumpled cloth. (2) cloth folding, where the task is to fold a piece of randomly positioned flattened cloth in half.

3) *Model Learning*: We split the training of G-DOOM into two phases. Firstly, we pre-train the Transporter network. Qualitatively, we find using $K = 8$ keypoints for cloth manipulation and $K = 3$ keypoints for rope straightening performs well. Next, we freeze the weights of the Transporter and train the dynamics model. For a fair comparison, we train all baselines with the same number of epochs.

4) *Evaluation Setups*: In all tasks, we allow a maximum sequence length of 20 steps and report the success rate over 1000 different random seeds. We define the success criteria as the distance to goal given the ground-truth particle locations in the simulator. For the *contrastive learning methods* (G-DOOM and CFM), we also report the top 1 prediction accuracy [7]. This is computed by unrolling the dynamics model for 20 steps, and measure the prediction error $d(\hat{s}_t, s_t)$ between the predicted state \hat{s}_t and the encoded state s_t , against N negative samples $\{s_j\}_{j=1}^J$. The top 1 accuracy is computed by $Acc = 1/N \sum_{n=1}^N \mathbb{I}(\forall j, d(\hat{s}_t^n, s_t^n) < d(\hat{s}_t^n, s_j^n))$.

B. Simulation Experiment

We present the highest reward achieved in Tab. I and the dynamics accuracy for in Tab. II. We observe that:

Graph dynamics better captures complex dynamics. In all cases, G-DOOM achieves the highest success rate. It suggests that the graph-based dynamics generally improve the quality of the learned dynamics model and the overall performance, compared to the single-vector-based dynamics. Besides, the advantage of G-DOOM is clearer on cloth manipulation tasks than the simpler rope straightening tasks. This further emphasizes the benefit of graph structure in the dynamics.

Belief tracking is necessary for complex dynamics. Both PlaNet and G-DOOM perform belief tracking with an additional hidden vector using RNNs, while CFM is state-dependent, *i.e.*, remembers no history. In most of the cases, CFM performs worse than PlaNet and G-DOOM, which is contradictory to the original results of the CFM paper [35]. The reason is that originally, CFM allows a longer execution sequence length with a smaller step size: 40 steps are allowed for rope straightening and 100 steps are allowed for cloth manipulation. However, in our case, larger step size is used with a much shorter time limit: 20 steps for all tasks, which leads to more complex dynamics. Besides, the masked depth images contain fewer

TABLE I
SIMULATION EXPERIMENTS: SUCCESS RATE (%)

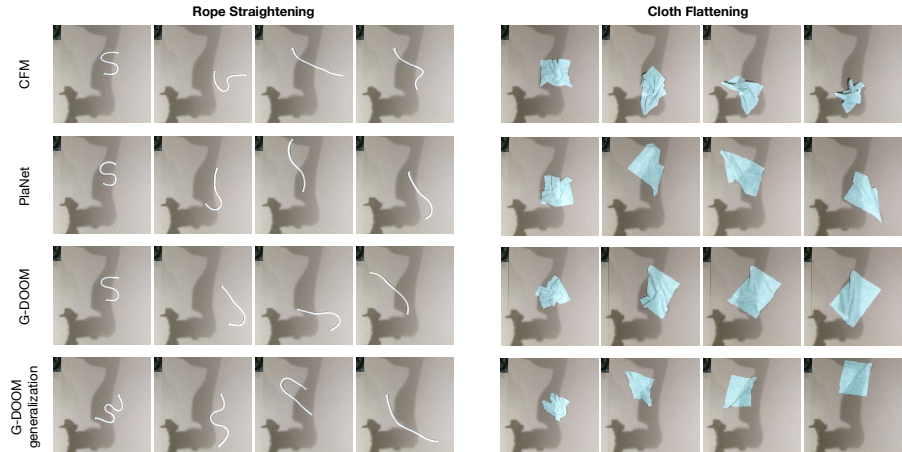
	Rope				Cloth	
	0°	45°	90°	135°	Flatten	Fold
CFM	24.7	18.4	9.1	11.6	29.2	59.6
PlaNet	39.1	68.1	64.4	82.4	35.9	73.2
G-DOOM	65.7	80.3	73.2	98.1	95.1	92.5

TABLE II
SIMULATION EXPERIMENTS: PREDICTIVE DYNAMICS ACCURACY (%)

	Rope				Cloth	
	0°	45°	90°	135°	Flatten	Fold
CFM	47.7	44.8	48.4	49.6	59.4	61.1
PlaNet	-	-	-	-	-	-
G-DOOM	99.9	99.9	99.8	99.9	99.9	99.9



(a)



(b)

Fig. 4. Robot experiments on rope straightening (135°) and cloth flattening. (a) We use a Kinova Gen3 robot with a Robotiq hand for manipulation and a Kinect 2.0 camera with a top-down view for depth sensing. (b) We show the execution trajectory of each method (CFM, PlaNet, and G-DOOM) on the two tasks over 4 time steps. G-DOOM generalization (bottom row) shows that the learned G-DOOM model generalizes to different initial configurations or different object variants, e.g., a longer rope and a smaller piece of cloth.

signals (most of the pixels are 0), which makes it difficult for pure contrastive learning methods.

G-DOOM learns a more robust contrastive dynamics model. We measure the *dynamics accuracy*, which is 1 if the positive state-observation pair produces the lowest L2 distance, compared with other 50 negative samples [35]. In Tab. II, CFM achieves a low dynamics accuracy, while G-DOOM achieves almost 100% accuracy. This explains the low success rate of CFM. G-DOOM focuses on keypoints and learns a better dynamics model with the recurrent graph dynamics.

C. Real Robot Experiment

We evaluate our learned model on a Kinova Gen3 robot, as shown in Fig. 4a. To collect high-quality depth images, we mount a top-down Kinect 2.0 camera over the workspace. We observe that high-quality depth images and the simplified pick-and-place action model help to minimize the sim-to-real gap, and our trained models transfer directly to the real robot.

Evaluation metric: We measure the distance-to-goal by counting the number of pixels within a goal region. Denoting the set of pixels covered by a deformable object as S_o , we define the score as follows. For rope straightening tasks, we define goal region S_g to be a rectangle centered in the middle of the image rotated for different degrees (0°, 45°, 90°, 135°), and measure score = $|S_o \cap S_g|$; for cloth flattening, we simply compute the total number of pixels of the covered area by score = $|S_o|$; for cloth folding, we define the goal area to be half of the cloth

TABLE III
REAL ROBOT EXPERIMENT RESULTS

	Rope				Cloth	
	0°	45°	90°	135°	Flatten	Fold
CFM	1.378	33.26	45.64	14.49	515.24	-158.15
PlaNet	40.93	68.52	36.92	11.51	946.82	-199.08
G-DOOM	81.91	67.56	47.92	53.50	1,458.15	-42.15

in the initial frame and measure score = $-||S_o| - |S_g||$. All results are averaged over 3 random seeds.

Results: The quantitative results of the real robot experiments are given in Tab. III and visualizations are provided in Fig. 4.

G-DOOM generally outperforms the baselines. In real robot experiments, G-DOOM achieves higher scores than the baselines, which is consistent with our simulation results.

Graph-based dynamics allow G-DOOM to generalize better. In the simulation, PlaNet achieves reasonable performance on rope straightening tasks, while on a real robot, it fails on rope straightening 0° and 135°. In contrast, G-DOOM generalizes in all cases. This is because by down-sampling an object into a keypoint-based graph, G-DOOM constructs an information bottleneck that filters the high-frequency noise and maintains a minimum amount of information for modeling the dynamics. Also, the recurrent graph dynamics compensate for the information loss. As shown in Fig. 4b G-DOOM (generalization), our trained model can be directly applied to different objects, e.g., longer ropes and smaller cloths. Due

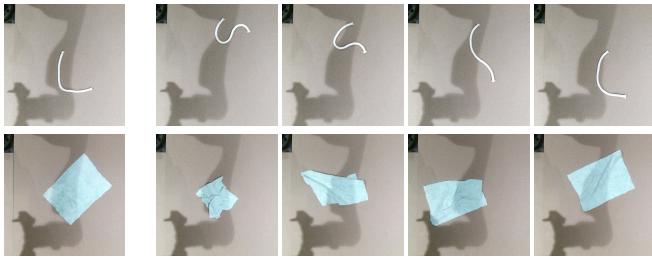


Fig. 5. G-DOOM performs goal-directed manipulation with a goal image as the input (first column).

to the space limit, we visualize two real-robot tasks in Fig. 4b.

D. Additional Qualitative Results

As discussed in Sect. III-B2, G-DOOM can also be used to perform the goal-directed manipulation with the contrastively learned dynamics. We provide qualitative results of this in Fig. 5. With an image of a “L”-shaped rope or an image of a piece of flattened cloth as the input, G-DOOM can successfully position the rope and cloth to the target configuration. However, we also noticed that it remains difficult for the goal-oriented policy to tackle tasks that require careful 3D understanding, *e.g.*, cloth folding. This is because the 2D goal image provides no 3D understanding of the task. We leave it for future study. We also visualize the learned keypoints (Fig 6) in both simulation and real-robot experiments. Because of the use of depth sensing, the sim-to-real gap is moderate, and we can reliably detect keypoints in both cases.

E. Ablation Study

We conduct an extensive ablation study to understand the influence of each proposed G-DOOM component (Tab. IV).

Imposing a graph structure in the dynamics model generally improves the performance of the algorithm. Compared with the standard G-DOOM, the NoGraph variant removes the graph-based representation and dynamics. We observe that G-DOOM generally outperforms the NoGraph variant in all tasks, which suggests that the graph-based representation better captures the dynamics of a deformable object.

Belief tracking with RNN is necessary to handle partial observability. The NoRNN variant removes the RNN and directly uses a single TGConv as the transition function f_{gmn} . We observe that NoRNN achieves reasonable performance on rope straightening tasks, while on cloth manipulation where partial observability exists, its performance degrades. It suggests that belief-tracking with a RNN is useful to tackle the self-occlusions in cloth manipulation tasks.

Hinge-loss-based contrastive learning improves the robustness of the learned dynamics model. The NoContrastive variant of G-DOOM removes the contrastive component in loss function Eqn. 5 and minimizes only the difference between the true states and predicted states. Also, the InfoNCE variant replaces the hinge loss with the standard InfoNCE [20] used in CFM. They perform generally worse than G-DOOM, which suggests contrastive learning is necessary, and hinge loss improves the robustness of the model.

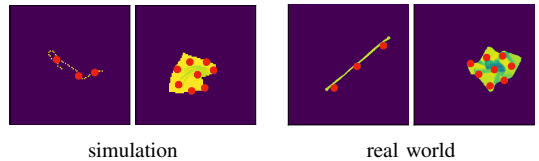


Fig. 6. Keypoint detections in simulation and real-robot experiments.

TABLE IV
ABLATION STUDY: SUCCESS RATE (%)

	Rope				Cloth	
	0°	45°	90°	135°	Flatten	Fold
NoGraph	7.2	5.7	4.1	34.4	75.8	64.1
NoRNN	34.1	37.7	69.3	84.1	78.7	22.9
NoContrastive	0.2	0.7	3.8	5.5	29.7	29.7
InfoNCE	3.5	69.4	26.8	9.2	31.0	61.9
CEM	25.0	72.0	39.0	33.6	91.9	58.5
GAT	13.2	9.4	28.3	31.7	37.7	28.3
MaxPool	28.1	31.9	29.9	65.5	94.8	55.7
G-DOOM	65.7	80.3	73.2	98.1	95.1	92.5

Graph-based CEM can improve the search performance. The CEM variant replaces the Graph-based CEM with a standard CEM, without using the keypoint positions as a prior to initialize the search. As a result, given the same number of optimization iterations, the standard CEM shows worse performance than the original G-DOOM.

TGConv improves the spatial modeling ability for a deformable object. The GAT variant of G-DOOM replaces the TGConv graph convolution by the widely adopted Graph Attention Networks (GAT) [30]. After replacing the TGConv with GAT, we observe that the overall performance of G-DOOM generally degrades, which is because using the relatively simple GAT is insufficient to model the complex spatio-temporal microscopic interaction of a deformable object.

MGF features improve the global feature extraction of a graph. The MaxPool variant of G-DOOM replaces the MGF features for global feature extraction by the MaxPooling technique generally used in point cloud learning literature [21, 22]. G-DOOM with MGF features generally gives a higher success rate than the MaxPool variant.

V. CONCLUSION

G-DOOM performs visual manipulation of deformable objects. Instead of modeling the full dynamics, it learns a recurrent graph dynamics model over the keypoints, detected automatically from images, and uses the learned model to plan manipulation actions. The encouraging experimental results support an interesting finding: a sparse set of keypoints can capture the dynamics of a complex deformable object for manipulation planning.

At the same time, G-DOOM is the first attempt and currently has various limitations. The rope and cloth manipulation tasks attempted so far involve relatively simple and smooth dynamics. To tackle complex tasks, such as knot tying or Japanese T-shirt folding, we need more powerful dynamics models learned on much larger datasets as well as long-horizon planning methods.

REFERENCES

- [1] Siwei Chen, Xiao Ma, Yunfan Lu, and David Hsu. Ab initio particle-based object manipulation. *arXiv preprint arXiv:2107.08865*, 2021.
- [2] Gianni Ciccarelli. Particle-based fluid simulation with nvidia flex. 2019.
- [3] Aditya Ganapathi, Priya Sundaesan, Brijen Thananjeyan, Ashwin Balakrishna, Daniel Seita, Jennifer Grannen, Minh Hwang, Ryan Hoque, Joseph E Gonzalez, Nawid Jamali, et al. Learning dense visual correspondences in simulation to smooth and fold real fabrics. In *2021 IEEE International Conference on Robotics and Automation (ICRA)*, pages 11515–11522. IEEE, 2021.
- [4] Danijar Hafner, Timothy P. Lillicrap, Ian Fischer, Ruben Villegas, David Ha, Honglak Lee, and James Davidson. Learning latent dynamics for planning from pixels. In Kamalika Chaudhuri and Ruslan Salakhutdinov, editors, *Proceedings of the 36th International Conference on Machine Learning, ICML 2019, 9-15 June 2019, Long Beach, California, USA*, volume 97 of *Proceedings of Machine Learning Research*, pages 2555–2565. PMLR, 2019. URL <http://proceedings.mlr.press/v97/hafner19a.html>.
- [5] Shervin Javdani, Siddhartha S Srinivasa, and J Andrew Bagnell. Shared autonomy via hindsight optimization. *Robotics science and systems: online proceedings*, 2015, 2015.
- [6] Peter Karkus, Xiao Ma, David Hsu, Leslie Pack Kaelbling, Wee Sun Lee, and Tomás Lozano-Pérez. Differentiable algorithm networks for composable robot learning. *Robotics: Science and Systems*, 2019.
- [7] Thomas N. Kipf, Elise van der Pol, and Max Welling. Contrastive learning of structured world models. In *8th International Conference on Learning Representations, ICLR 2020, Addis Ababa, Ethiopia, April 26-30, 2020*. OpenReview.net, 2020. URL <https://openreview.net/forum?id=H1gax6VtDB>.
- [8] Tejas D Kulkarni, Ankush Gupta, Catalin Ionescu, Sebastian Borgeaud, Malcolm Reynolds, Andrew Zisserman, and Volodymyr Mnih. Unsupervised learning of object keypoints for perception and control. *Advances in neural information processing systems*, 32:10724–10734, 2019.
- [9] Robert Lee, Daniel Ward, Akansel Cosgun, Vibhavari Dasagi, Peter Corke, and Jurgen Leitner. Learning arbitrary-goal fabric folding with one hour of real robot experience. *Conference on Robot Learning*, 2020.
- [10] Yinxiao Li, Yonghao Yue, Danfei Xu, Eitan Grinspun, and Peter K Allen. Folding deformable objects using predictive simulation and trajectory optimization. In *2015 IEEE/RSJ International Conference on Intelligent Robots and Systems (IROS)*, pages 6000–6006. IEEE, 2015.
- [11] Yunzhu Li, Jiajun Wu, Russ Tedrake, Joshua B. Tenenbaum, and Antonio Torralba. Learning particle dynamics for manipulating rigid bodies, deformable objects, and fluids. In *7th International Conference on Learning Representations, ICLR 2019, New Orleans, LA, USA, May 6-9, 2019*. OpenReview.net, 2019. URL <https://openreview.net/forum?id=rJgbSn09Ym>.
- [12] Xingyu Lin, Yufei Wang, Jake Olkin, and David Held. Softgym: Benchmarking deep reinforcement learning for deformable object manipulation. *arXiv preprint arXiv:2011.07215*, 2020.
- [13] Xingyu Lin, Yufei Wang, and David Held. Learning visible connectivity dynamics for cloth smoothing. *arXiv preprint arXiv:2105.10389*, 2021.
- [14] Xiao Ma, Siwei Chen, David Hsu, and Wee Sun Lee. Contrastive variational model-based reinforcement learning for complex observations. *arXiv preprint arXiv:2008.02430*, 2020.
- [15] Xiao Ma, Péter Karkus, David Hsu, and Wee Sun Lee. Particle filter recurrent neural networks. In *The Thirty-Fourth AAAI Conference on Artificial Intelligence, AAAI 2020*, pages 5101–5108. AAAI Press, 2020.
- [16] Jan Matas, Stephen James, and Andrew J Davison. Sim-to-real reinforcement learning for deformable object manipulation. In *Conference on Robot Learning*, pages 734–743. PMLR, 2018.
- [17] Stephen Miller, Jur Van Den Berg, Mario Fritz, Trevor Darrell, Ken Goldberg, and Pieter Abbeel. A geometric approach to robotic laundry folding. *The International Journal of Robotics Research*, 31(2):249–267, 2012.
- [18] Volodymyr Mnih, Adrià Puigdomènech Badia, Mehdi Mirza, Alex Graves, Timothy P. Lillicrap, Tim Harley, David Silver, and Koray Kavukcuoglu. Asynchronous methods for deep reinforcement learning. In Maria-Florina Balcan and Kilian Q. Weinberger, editors, *Proceedings of the 33rd International Conference on Machine Learning, ICML, 2016*.
- [19] Mark Moll and Lydia E Kavraki. Path planning for deformable linear objects. *IEEE Transactions on Robotics*, 22(4):625–636, 2006.
- [20] Aaron van den Oord, Yazhe Li, and Oriol Vinyals. Representation learning with contrastive predictive coding. *arXiv preprint arXiv:1807.03748*, 2018.
- [21] Charles R Qi, Hao Su, Kaichun Mo, and Leonidas J Guibas. Pointnet: Deep learning on point sets for 3d classification and segmentation. In *Proceedings of the IEEE conference on computer vision and pattern recognition*, pages 652–660, 2017.
- [22] Charles R Qi, Li Yi, Hao Su, and Leonidas J Guibas. Pointnet++: Deep hierarchical feature learning on point sets in a metric space. *arXiv preprint arXiv:1706.02413*, 2017.
- [23] Mitul Saha and Pekka Isto. Manipulation planning for deformable linear objects. *IEEE Transactions on Robotics*, 23(6):1141–1150, 2007.
- [24] Alvaro Sanchez-Gonzalez, Jonathan Godwin, Tobias Pfaff, Rex Ying, Jure Leskovec, and Peter Battaglia. Learning to simulate complex physics with graph networks. In *International Conference on Machine Learning*, pages 8459–8468. PMLR, 2020.
- [25] Daniel Seita, Aditya Ganapathi, Ryan Hoque, Minh

- Hwang, Edward Cen, Ajay Kumar Tanwani, Ashwin Balakrishna, Brijen Thananjeyan, Jeffrey Ichnowski, Nawid Jamali, et al. Deep imitation learning of sequential fabric smoothing policies. *arXiv preprint arXiv:1910.04854*, 2019.
- [26] Daniel Seita, Pete Florence, Jonathan Tompson, Erwin Coumans, Vikas Sindhwani, Ken Goldberg, and Andy Zeng. Learning to rearrange deformable cables, fabrics, and bags with goal-conditioned transporter networks. *arXiv preprint arXiv:2012.03385*, 2020.
- [27] Jerzy Smolen and Alexandru Patriciu. Deformation planning for robotic soft tissue manipulation. In *2009 Second International Conferences on Advances in Computer-Human Interactions*, pages 199–204. IEEE, 2009.
- [28] Eric Torgerson and Frank W Paul. Vision-guided robotic fabric manipulation for apparel manufacturing. *IEEE Control Systems Magazine*, 8(1):14–20, 1988.
- [29] Ashish Vaswani, Noam Shazeer, Niki Parmar, Jakob Uszkoreit, Llion Jones, Aidan N Gomez, Lukasz Kaiser, and Illia Polosukhin. Attention is all you need. *arXiv preprint arXiv:1706.03762*, 2017.
- [30] Petar Veličković, Guillem Cucurull, Arantxa Casanova, Adriana Romero, Pietro Lio, and Yoshua Bengio. Graph attention networks. *arXiv preprint arXiv:1710.10903*, 2017.
- [31] Takahiro Wada, Shinichi Hirai, Sadao Kawamura, and Norimasa Kamiiji. Robust manipulation of deformable objects by a simple pid feedback. In *Proceedings 2001 ICRA. IEEE International Conference on Robotics and Automation (Cat. No. 01CH37164)*, volume 1, pages 85–90. IEEE, 2001.
- [32] Yilin Wu, Wilson Yan, Thanard Kurutach, Lerrel Pinto, and Pieter Abbeel. Learning to manipulate deformable objects without demonstrations. *arXiv preprint arXiv:1910.13439*, 2019.
- [33] Zonghan Wu, Shirui Pan, Fengwen Chen, Guodong Long, Chengqi Zhang, and S Yu Philip. A comprehensive survey on graph neural networks. *IEEE transactions on neural networks and learning systems*, 32(1):4–24, 2020.
- [34] Yuji Yamakawa, Akio Namiki, and Masatoshi Ishikawa. Motion planning for dynamic folding of a cloth with two high-speed robot hands and two high-speed sliders. In *2011 IEEE International Conference on Robotics and Automation*, pages 5486–5491. IEEE, 2011.
- [35] Wilson Yan, Ashwin Vangipuram, Pieter Abbeel, and Lerrel Pinto. Learning predictive representations for deformable objects using contrastive estimation. *arXiv preprint arXiv:2003.05436*, 2020.
- [36] Cunjun Yu, Xiao Ma, Jiawei Ren, Haiyu Zhao, and Shuai Yi. Spatio-temporal graph transformer networks for pedestrian trajectory prediction. In *European Conference on Computer Vision*, pages 507–523. Springer, 2020.
- [37] Andy Zeng, Pete Florence, Jonathan Tompson, Stefan Welker, Jonathan Chien, Maria Attarian, Travis Armstrong, Ivan Krasin, Dan Duong, Vikas Sindhwani, et al. Transporter networks: Rearranging the visual world for robotic manipulation. *arXiv preprint arXiv:2010.14406*, 2020.